AN ABSTRACT OF THE THESIS OF

ANTON POLENSEK (Name) for the MASTER OF SCIENCE (Degree)

in CIVIL ENGINEERING (Major) presented on August 26, 1968 (Date)

Title: FREQUENCY ANALYSIS OF TIMBER-JOIST FLOORS

Abstract approved: Redacted for Privacy
John Peterson

Matrix formulation was combined with the Bleich method of frequency analysis to determine the natural frequencies of timber-joist floors. Determination of the frequency equation expressed in matrix form involved the development and the formulation of the following three matrices for the statically determinate primary system: $\underset{\sim}{a}$ on the basis of internal virtual moments, $\underset{\sim}{\beta}$ on the basis of modal deflections and virtual displacements, and $\underset{\sim}{\omega}_I$ on the basis of natural frequencies.

The frequency equation was solved by the use of a high speed digital computer. Calculated values agreed closely with the test values.

Frequency Analysis of Timber-Joist Floors

by

Anton Polensek

A THESIS

submitted to

Oregon State University

in partial fulfillment of
the requirements for the
degree of

Master of Science

June 1969

APPROVED:

Redacted for Privacy

Associate Professor of Civil Engineering

in charge of major

Redacted for Privacy

Head of Department of Civil Engineering

Redacted for Privacy

Dean of Graduate School

Date thesis is presented August 26, 1968

Typed by Clover Redfern for Anton Polensek

ACKNOWLEDGMENTS

The author wishes to express appreciation for the advice and assistance of Dr. John Peterson of the Civil Engineering Department. Dr. Harold I. Laursen of the same department also gave helpful suggestions and Mr. Jay R. Murray of the Computer Center provided the computer programming.

TABLE OF CONTENTS

LIST OF FIGURES

LIST OF APPENDIX TABLES

FREQUENCY ANALYSIS OF TIMBER-JOIST FLOORS

INTRODUCTION

One of the reasons for deflection limitations on floor structures given in current building codes is to provide the necessary stiffness to reduce vibrations below a limit that humans can tolerate (13, p. 20-25). As early as 1931, tests conducted in Germany established a direct relationship between human vibratory perceptibility and the frequency and amplitude of undamped sinusoidal oscillations (12, p. 3-8). Since then, numerous studies have been conducted in order to relate human vibration response to structural dynamic parameters such as frequency, amplitude, acceleration and damping (11, p. 1, 6). Any form of dynamic loading such as falling objects, people and animals walking, etc., force the floor structure to oscillate in its natural modal shapes and frequencies (7, p. 9-11). The response to such a loading may be a simple free vibration, induced perhaps by a fallen object, or a more complex response termed random vibration, induced perhaps by several people walking simultaneously on the floor.

Structures loaded with dynamic forces of random or periodic occurrence must possess such stiffness and mass distribution that their significant modal frequencies differ from those generated by the loading. If not, resonant effect can cause stresses of a magnitude far

beyond the value resulting from static loading.

Whether a structural designer is concerned with the problem of vibrations as they may occur in a residential building, or as may be caused by rotating machinery and other moving apparatus in a commercial structure, or the effect of earthquake ground motion on all types of buildings, he has to establish the contributing natural modal shapes and frequencies of the structural system.

REVIEW OF THE MOST IMPORTANT METHODS OF FREQUENCY ANALYSIS

Determination of Natural Frequency by Solving Equations of Motion

The frequency equation developed from differential equations of motion is a polynomial equation of degree n where n is the number of masses in the vibrating system (2, p. 89-91). The frequency equation of frictionless systems yields real roots, while the solution for systems with damping consists of conjugate complex roots. Exact procedures of solving polynomial equations such as Graeffe's method are time-consuming and impractical when n becomes large (8, p. 527). However, application of high-speed digital computers in structural analysis during recent years has made these methods more attractive.

Approximate Methods Derived from Equations of Motion

In this category there are several methods, of which those listed are the ones most commonly found in the literature.

The Stodola-Vianello Method

This method is the most widely used numerical procedure to solve equations of motion to establish the natural frequencies and characteristic modal shapes (2, p. 97-101). Its application is limited

to systems having relatively few degrees of freedom.

Dunkerley's Formula

This formula gives an approximate value of the fundamental frequency which is always lower than the true value. Such a value may be further refined by Newton's method of successive approximation or by matrix-iteration process (14, p. 189-197).

The Holzer Method

This method is commonly used for analyzing torsional vibrating systems. It is a trial-and-error method based on the equilibrium equations (14, p. 201-205).

Energy Methods

Energy methods are based on the principle of periodic exchange of kinetic and potential energies of a freely vibrating, frictionless system. The most important method is the Rayleigh procedure, in which the frequency of the fundamental mode is obtained by equating the maximum potential and kinetic energies of the vibrating system (2, p. 105-111). The calculation is based on the assumed shape of a dynamic deflection curve for the structure. The method yields basic frequencies which are equal to or higher than the exact values. The closer the assumed curve to the system's true shape, the closer the

calculated frequency will be to its true value. The errors in the assumed deflection curve have small effect on the deviation of the resulting frequency from its real value as long as the assumed curve does not violate the boundary conditions of the system (8, p. 71, 72, 120, 121).

Bleich's Method

This method yields exact values of the natural frequencies even when the system is of a highly complex nature (3, p. 1023-1041). It is based on compatibility conditions. The procedure yields a polynomial frequency equation similar to that obtained from equations of motion, but it allows the more complex structure to be transformed into simpler sub-systems which are analyzed individually and then recombined into the original system.

SYSTEM AND NOTATIONS

The type of structure analyzed is a typical timber-joist floor system, constructed according to the provisions of the Uniform Building Code (6, Sec. 2509). The geometry and notation of the system are shown in Figure 1. The floor superstructure hereinafter called floor is considered to be fastened to the joists so that the vertical forces can be transferred between both parts, but the parts do not form one composite unit.

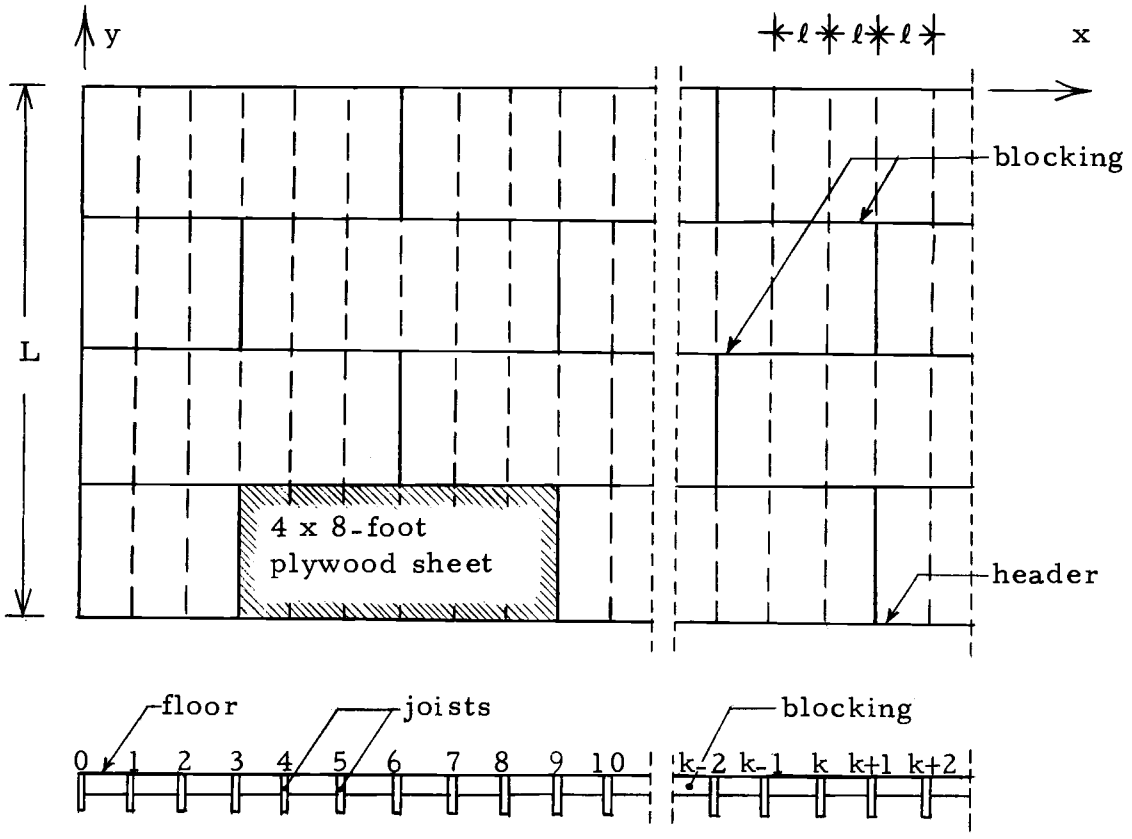

Figure 1. Layout of timber-joist floor system.

ASSUMPTIONS

In the following analysis, the assumptions made are:

1. The system oscillates in the elastic range
2. Damping is not included in the calculation
3. The contribution of blocking and headers to the distribution of forces in the direction across the joists is ignored
4. Rigidity and mass distribution are constant along each joist
5. Rigidity and mass distribution per unit area of floor are constant.

METHOD OF ANALYSIS

The method of frequency analysis applied was developed by Hans H. Bleich (3, p. 1030-1032, 1039-1041). The notation is the same as used by Bleich except that the matrix formulation is used.

The analysis is performed in two steps:

a. Determination of the frequency and modal shapes of a statically determinate primary system

b. Influence of the redundancy added to the above analysis.

Frequency and Modal Shape of the Primary System

The complex floor system is initially transformed into a statically determinate primary system (i. e., comprised of a series of simple beams) by releasing the continuity moments in the floor where it crosses the joists. Exact values of frequencies and shapes of such a system can be determined by the method which Bleich developed for solving statically determinate structures (3, p. 1026-1035).

To avoid cumbersome calculations associated with solving of the polynomial equation required by the above method, the floor mass is proportionally added to the joist masses, thus generating a primary system consisting of simple beams. Errors caused by such a simplification are small if the following requirements are met (3, p. 1036, 1037):

1. The relative rigidity of the floor must be large in comparison to that of the joists. The span of floor superstructure "ℓ" is much smaller than the joist span "L". For this reason, the relative mid-span deflection of the floor due to self weight is only a fraction of the corresponding deflection of the joist. Therefore, the floor simply follows the paths of the joists, and its modal participation factors are of very low magnitude.
2. The system should have more than two joists.
3. Exact frequencies of higher modes are not required. This method gives a very accurate basic frequency but only approximate values for higher modes. In this calculation only basic modes of individual joists will be considered. Higher modes could be important only in a few special cases of forced vibration.

The modal shapes and frequencies based on a simple beam calculation are given by (3, p. 1041)

$$\phi_i = \sqrt{\frac{2}{m_k' L}} \sin \frac{i\pi y}{L} \tag{1}$$

and

$$\omega_i = \frac{i^2 \pi^2}{L^2} \sqrt{\frac{E_k I_k}{m_k'}} \tag{2}$$

where terms are defined as follows:

ϕ is modal shape,

ω is circular frequency, radians per second,

i is mode, i = 1, 2, 3, . . . ,

k is location of joist and nodal location respectively,

E is modulus of elasticity, lb/in^2,

I is moment of inertia, in^4 and

m_k' is uniformly distributed mass of joist k which includes the proportionate weight of the floor, $lb\ sec/in^2$.

Development of the Frequency Equation

The effect of the action of redundant moments on a statically determinate primary system is described by the following two equations as developed by Bleich (3, Equations 43 and 49):

$$(\frac{\omega_i^2}{\omega^2} - 1)c_i = \sum_k \beta_{i,k} X_k \tag{3}$$

and

$$\sum_i \omega_i^2 \beta_{i,j} c_i + \sum_k \alpha_{j,k} X_k = 0 \tag{4}$$

where

$$\beta_{i,k} = \int_m \phi_i \psi_k dm \tag{5}$$

and

$$\alpha_{j,k} = \int_s EI\ddot{\psi}_j \ddot{\psi}_k ds = \int \overline{m}_j \overline{m}_k \frac{ds}{EI} \tag{6}$$

Terms are defined as follows:

ω_i is defined by Equation 2,

ω is frequency of the floor system,

c_i is modal amplitude (2, p. 331),

X_k is redundant moment at k,

ϕ_i is defined by Equation 1,

ψ_k is deflection of a primary system due to virtual moment applied at k,

m is mass,

$\ddot{\psi}_k = \frac{d^2\psi_k}{ds^2} = -\frac{\overline{m}_k}{EI}$ where $\overline{m}_k$ is internal virtual moment in a primary system, and

j is nodal location.

Equations 3 and 4 may be written in matrix formulation as

$$\underset{\sim}{\overline{\omega}}\,\underset{\sim}{c} = \underset{\sim}{\beta X} \tag{7}$$

and

$$\underset{\sim}{\beta'}\,\underset{\sim}{\omega_I}\,\underset{\sim}{c} = \underset{\sim}{a X} \tag{8}$$

where

$$\underset{\sim}{\overline{\omega}} = \begin{bmatrix} \frac{\omega_1^2}{\omega^2} - 1 & & & \\ & \frac{\omega_2^2}{\omega^2} - 1 & & \\ & & \ddots & \\ & & & \frac{\omega_n^2}{\omega^2} - 1 \end{bmatrix} \tag{7a}$$

$$\underset{\sim}{c} = \begin{bmatrix} c_1 \\ c_2 \\ \cdots \\ c_n \end{bmatrix} \tag{7b}$$

$$\underset{\sim}{\beta} = \begin{bmatrix} \beta_{11} & \beta_{12} & \cdots & \beta_{1n} \\ \beta_{21} & \beta_{22} & \cdots & \beta_{2n} \\ \cdots & \cdots & \cdots & \cdots \\ \beta_{n1} & \beta_{n2} & \cdots & \beta_{nn} \end{bmatrix} \tag{7c}$$

$\underset{\sim}{\beta}'$ is the transpose of $\underset{\sim}{\beta}$,

$$\underset{\sim}{X} = \begin{bmatrix} X_1 \\ X_2 \\ \cdots \\ X_n \end{bmatrix} \tag{7d}$$

$$\underset{\sim}{\omega}_I = \begin{bmatrix} \omega_1^2 & & & \\ & \omega_2^2 & & \\ & & \cdots & \\ & & & \omega_n^2 \end{bmatrix} \tag{8a}$$

and

$$\underset{\sim}{a} = \begin{bmatrix} a_{11} & a_{12} & \cdots & a_{1n} \\ a_{21} & a_{22} & \cdots & a_{2n} \\ \cdots & \cdots & \cdots & \cdots \\ a_{n1} & a_{n2} & \cdots & a_{nn} \end{bmatrix} \tag{8b}$$

The symbol n is the number of participating modes of the primary system. Since the modes of a primary system are the basic modes for the individual joists, and since redundant moments also occur at each joist, n also equals the number of redundant moments. Thus $\underset{\sim}{\alpha}$ and $\underset{\sim}{\beta}$ must be square matrices.

Equation 8 may be written:

$$\underset{\sim}{X} = \underset{\sim}{\alpha}^{-1}\underset{\sim}{\beta}'\underset{\sim}{\omega}_I\underset{\sim}{c} \tag{8c}$$

Substituting Equation 8c into Equation 7 gives

$$\underset{\sim}{\bar{\omega}}\,\underset{\sim}{c} - \underset{\sim}{\beta\alpha}^{-1}\underset{\sim}{\beta}'\underset{\sim}{\omega}_I\underset{\sim}{c} = \underset{\sim}{0} \tag{9}$$

where $\underset{\sim}{0}$ is a null vector

and $$(\underset{\sim}{\bar{\omega}} - \underset{\sim}{\beta\alpha}^{-1}\underset{\sim}{\beta}'\underset{\sim}{\omega}_I)\underset{\sim}{c} = \underset{\sim}{0} \tag{9a}$$

Matrix $\underset{\sim}{\bar{\omega}}$ may be written as

$$\underset{\sim}{\bar{\omega}} = \underset{\sim}{\bar{\bar{\omega}}} - \underset{\sim}{I} \tag{10}$$

where $\underset{\sim}{I}$ is identity matrix

and

$$\underset{\sim}{\bar{\bar{\omega}}} = \begin{bmatrix} \frac{\omega_1^2}{\omega^2} & & & \\ & \frac{\omega_2^2}{\omega^2} & & \\ & & \cdots & \\ & & & \frac{\omega_n^2}{\omega^2} \end{bmatrix} = \left(\frac{1}{\omega^2}\right)\underset{\sim}{\omega}_1 \tag{11}$$

Substituting Equations 10 and 11 into Equation 9a gives

$$(\frac{1}{\omega^2}\,\underset{\sim}{\omega}_I - \underset{\sim}{I} - \underset{\sim}{\beta}\underset{\sim}{a}^{-1}\underset{\sim}{\beta}'\underset{\sim}{\omega}_I)\underset{\sim}{c} = \underset{\sim}{0} \tag{12}$$

Equation 12 is multiplied by scalar ω^2:

$$[\underset{\sim}{\omega}_I - (\underset{\sim}{I} + \underset{\sim}{\beta}\underset{\sim}{a}^{-1}\underset{\sim}{\beta}'\underset{\sim}{\omega}_I)\omega^2]\underset{\sim}{c} = \underset{\sim}{0} \tag{13}$$

Premultiplying Equation 13 by $(\underset{\sim}{I}+\underset{\sim}{\beta}\underset{\sim}{a}^{-1}\underset{\sim}{\beta}'\underset{\sim}{\omega}_I)^{-1}$ results in

$$[(\underset{\sim}{I} + \underset{\sim}{\beta}\underset{\sim}{a}^{-1}\underset{\sim}{\beta}'\underset{\sim}{\omega}_I)^{-1}\underset{\sim}{\omega}_I - \underset{\sim}{I}\omega^2]\underset{\sim}{c} = \underset{\sim}{0} \tag{14}$$

Equation 14 forms a set of linear and homogeneous equations for values $\underset{\sim}{c}$. Such equations have a nontrivial solution for $\underset{\sim}{c}$ only if the determinant of coefficients of vector $\underset{\sim}{c}$ equals zero.

Therefore

$$|(\underset{\sim}{I} + \underset{\sim}{\beta}\underset{\sim}{a}^{-1}\underset{\sim}{\beta}'\underset{\sim}{\omega}_I)^{-1}\underset{\sim}{\omega}_I - \omega^2\underset{\sim}{I}| = 0 \tag{15}$$

Equation 15 is a frequency equation of the floor system. It is expressed in a form which is suitable for computer solution.

Mathematical definitions and rules for matrices used in the preceding development are based on reference 9, p. 1-23.

Development of Matrix $\underset{\sim}{\beta}$

Equation 5 can be written in a matrix form:

$$\underset{\sim}{\beta} = \int_{m} \underset{\sim}{\phi}\underset{\sim}{\psi} dm \tag{16}$$

where

$$\underset{\sim}{\phi} = \begin{bmatrix} \phi_1 \\ \phi_2 \\ \cdots \\ \phi_n \end{bmatrix}$$

and

$$\underset{\sim}{\psi} = [\psi_1 \psi_2 \cdots \psi_n]$$

Therefore

$$\underset{\sim}{\beta} = \int_{m} \begin{bmatrix} \phi_1\psi_1 & \phi_1\psi_2 & \cdots & \phi_1\psi_n \\ \phi_2\psi_1 & \phi_2\psi_2 & \cdots & \phi_2\psi_n \\ \cdots & \cdots & \cdots & \cdots \\ \phi_n\psi_1 & \phi_n\psi_2 & \cdots & \phi_n\psi_n \end{bmatrix} dm = \begin{bmatrix} \beta_{11} & \beta_{12} & \cdots & \beta_{1n} \\ \beta_{21} & \beta_{22} & \cdots & \beta_{2n} \\ \cdots & \cdots & \cdots & \cdots \\ \beta_{n1} & \beta_{n2} & \cdots & \beta_{nn} \end{bmatrix} \tag{16a}$$

Figure 2 shows the virtual deflection of the primary system due to the action of the external virtual moment $X_k = 1$ in-lb/in. The functions indicated in the figure are defined as follows (10, p. 87-90):

$$\psi(y)_k = \frac{y^2 1b}{24EI_k \ell}(L^3 - 2Ly^2 + y^3) \tag{17a}$$

$$\psi(y)_{k-1} = \frac{y\,1b}{24EI_{k-1} \ell}(L^3 - 2Ly^2 + y^3) \tag{17b}$$

$$\psi(y)_{k+1} = \frac{y\,1b}{24EI_{k+1} \ell}(L^3 - 2Ly^2 + y^3) \tag{17c}$$

$$\psi(x)_{\overline{k-1}} = \frac{x}{\ell}\psi(y)_{k-1} \tag{17d}$$

$$\psi(x)_{\overline{k+2}} = \frac{x}{\ell}\psi(y)_{k+1} \tag{17e}$$

$$\psi(x)_{\overline{k}} = \psi(y)_{k-1} - [\psi(y)_{k-1} + |\psi(y)_k|]\frac{x}{\ell} + \frac{lb}{6EI_f}(\ell x - \frac{x^3}{\ell}) \tag{17f}$$

and

$$\psi(x)_{k+1} = \psi(y)_{k+1} - [\psi(y)_{k+1} + |\psi(y)_k|]\frac{x}{\ell} + \frac{lb}{6EI_f}(\ell x - \frac{x^3}{\ell}) \tag{17g}$$

Figure 3 shows the modal deflection of a primary system at nodal location k. Function $\phi(y)_k$ is defined by Equation 1.

Sign conventions shown in Figure 4 will be used throughout the calculation.

Based on Equation 5 and Figures 2 and 3,

$$\beta_{k,k} = \int_m \phi_k \psi_k dm = \left[\int_x \int_y \phi_k \psi_k dm\right]_{floor} + \left[\int_y \phi_k \psi_k dm\right]_{joists}$$

$$= \int_{x=0}^{\ell} \int_{y=0}^{L} \phi(y)_k (\frac{x}{\ell}) \{\psi(y)_{k-1} - [\psi(y)_{k-1} + |\psi(y)_k|]\frac{x}{\ell} + \psi(y)_{k+1}$$

$$- [\psi(y)_{k+1} + |\psi(y)_k|]\frac{x}{\ell} + 2[\frac{lb}{6EI_f}(\ell x - \frac{x^3}{\ell})]\} m_f dx dy + \int_{y=0}^{L} \phi(y)_k \psi(y)_k m_k dy \tag{18}$$

where

m_f is mass per unit of floor area,

m_k is mass of joist per linear length of joist,

$EI_k \equiv E_k I_k$ is rigidity of joist

and $EI_f \equiv E_f I_f$ is rigidity of a strip of floor one inch wide.

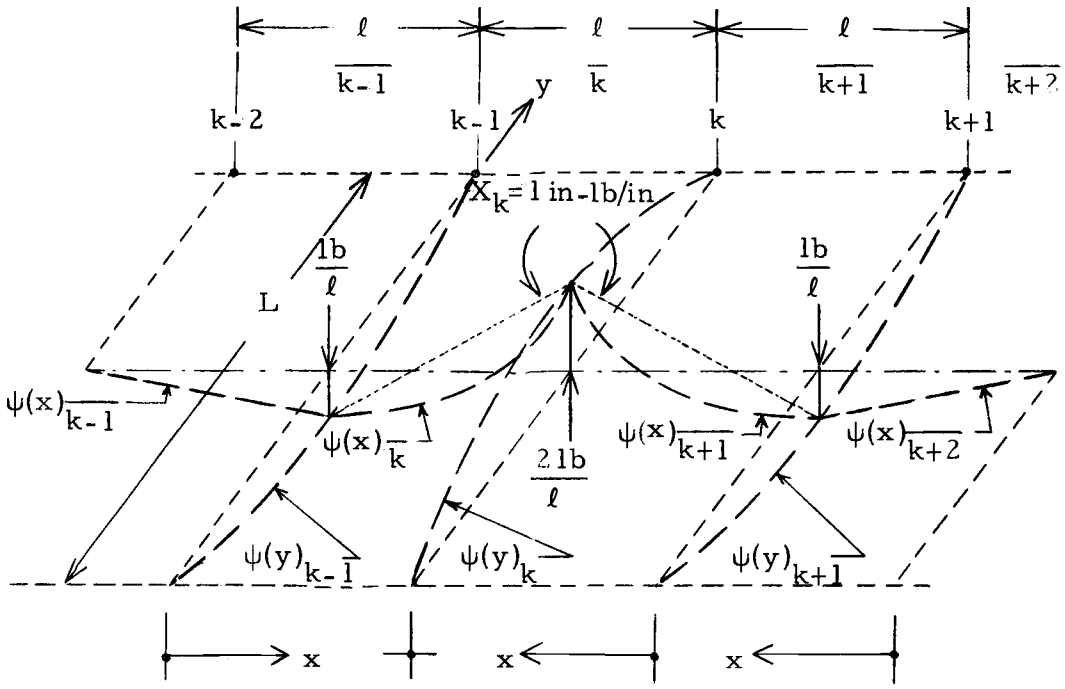

Figure 2. Displacement due to virtual moment X_k = 1 in-lb/in.

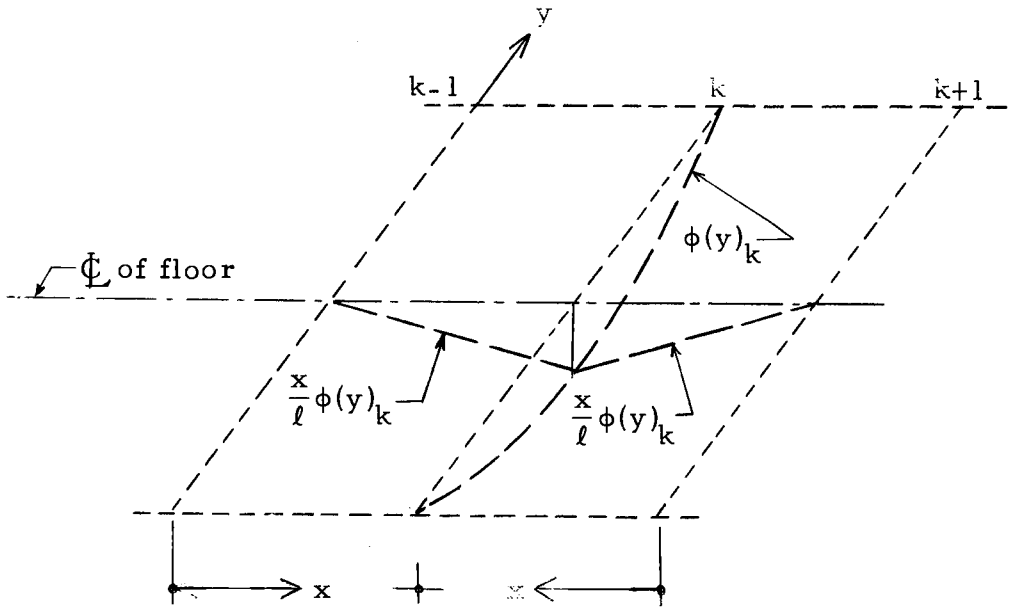

Figure 3. Modal displacement at the nodal location k.

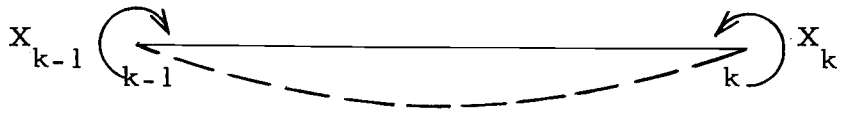

Figure 4. Sign convention.

Substituting Equations 17 into Equation 18 and performing integration gives the following final value of $\beta_{k,k}$[1]:

$$\beta_{k,k} = (9.242621)(10^{-3})(1b)\sqrt{\frac{L}{m_k'}}\left\{L^4\left[\frac{m_f}{6}\left(\frac{1}{EI_{k-1}}+\frac{1}{EI_{k+1}}-\frac{8}{EI_k}\right)-\frac{2m_k}{\ell EI_k}\right]\right.$$

$$\left. + 4.329265\,\frac{m_f \ell^3}{EI_f}\right\} \qquad (18a)$$

The following new terms are introduced:

$$B_{k,k+1} = b_k \frac{L^4 m_f}{6EI_{k+1}} \qquad (19a)$$

$$B_{k,k-1} = b_k \frac{L^4 m_f}{6EI_{k-1}} \qquad (19b)$$

$$B_{k,k} = b_k \frac{4L^4 \ell m_f - 6m_k}{3\ell EI_k} \qquad (19c)$$

and

$$B_{k,f} = b_k \frac{4.3293 m_f \ell^3}{EI_f} \qquad (19d)$$

[1] Refer to Appendix for development.

where

$$b_k = (9.242621)(10^{-3})\ lb\ \sqrt{\frac{L}{m_k'}}$$

Equations 19 are substituted into Equation 18a:

$$\beta_{k,k} = -[B_{k,k} - (B_{k,k+1} + B_{k,k-1} + B_{k,f})] \tag{18b}$$

The coefficient $\beta_{k,k+1}$ is determined in the same way as $\beta_{k,k}$ except that the virtual unit moment is applied at nodal location k+1, which translates virtual displacements in Figure 2 to the next nodal location on the right. Figure 2 applies if all the subscripts of the functions listed in the figure are increased by one. Figure 3 remains unchanged. The resulting expression is:

$$\beta_{k,k+1} = (9.242621)(10^{-3})(1b)\sqrt{\frac{L}{m_k'}}\left\{L^4\left[\left(\frac{2}{EI_k} - \frac{1}{EI_{k+1}}\right)\frac{m_f}{3} + \frac{m_k}{\ell EI_k}\right] + (0.5)(4.329265)\frac{m_f \ell^3}{EI_f}\right\} \tag{20}$$

or

$$\beta_{k,k+1} = 0.5(B_{k,k} - 4B_{k,k+1} + B_{k,f}) \tag{20a}$$

Similarly:

$$\beta_{k,k-1} = (9.242621)(10^{-3})(1b)\sqrt{\frac{L}{m_k'}}\left\{L^4\left[\left(\frac{2}{EI_k} - \frac{1}{EI_{k-1}}\right)\frac{m_f}{3} + \frac{m_k}{\ell EI_k}\right] + (0.5)(4.329265)\frac{m_f \ell^3}{EI_f}\right\} \tag{21}$$

or

$$\beta_{k,k-1} = 0.5(B_{k,k} - 4B_{k,k-1} + B_{k,f}) \tag{21a}$$

Coefficient $\beta_{k,k+2}$ is obtained in a similar way by integration over all the masses of the primary system for virtual displacement caused by virtual moment $X_{k+2} = 1$ in-lb/in and for modal displacement at the nodal location k. The expression thus obtained is

$$\beta_{k,k+2} = (9.242621)(10^{-3})(\text{lb})\left(\sqrt{\frac{L}{m_k'}}\right)\left(\frac{L^4 m_f}{6EI_{k+1}}\right) = B_{k,k+1} \tag{22}$$

Similarly:

$$\beta_{k,k-2} = (9.242621)(10^{-3})(\text{lb})\left(\sqrt{\frac{L}{m_k'}}\right)\left(\frac{L^4 m_f}{6EI_{k-1}}\right) = B_{k,k-1} \tag{23}$$

and

$$\beta_{k,j} = 0 \quad \text{if} \quad k + 3 \leq j \leq k - 3$$

The dimensions of coefficient β are $(\text{lb}^{1/2}\ \text{sec}\ \text{in}^{1/2})$.

Development of Matrix $\underset{\sim}{a}$

Equation 6 can be written in a matrix form:

$$\underset{\sim}{a} = \int_s \underset{\sim}{\overline{m}}' \underset{\sim}{\overline{m}} \frac{ds}{EI} \tag{24}$$

where $\underset{\sim}{\overline{m}} = [\overline{m}_1 \overline{m}_2 \ldots \overline{m}_n]$, $\underset{\sim}{\overline{m}}'$ is the transpose of $\underset{\sim}{\overline{m}}$, and s and EI are location variables.

Therefore

$$\underset{\sim}{a} = \int_s \begin{bmatrix} \overline{m}_1\overline{m}_1 & \overline{m}_1\overline{m}_2 & \cdots & \overline{m}_1\overline{m}_n \\ \overline{m}_2\overline{m}_1 & \overline{m}_2\overline{m}_2 & \cdots & \overline{m}_2\overline{m}_n \\ \cdots & \cdots & \cdots & \cdots \\ \overline{m}_n\overline{m}_1 & \overline{m}_n\overline{m}_2 & \cdots & \overline{m}_n\overline{m}_n \end{bmatrix} \frac{ds}{EI} = \begin{bmatrix} a_{11} & a_{12} & \cdots & a_{1n} \\ a_{21} & a_{22} & \cdots & a_{2n} \\ \cdots & \cdots & \cdots & \cdots \\ a_{n1} & a_{n2} & \cdots & a_{nn} \end{bmatrix} \tag{24a}$$

Figure 5 shows internal virtual moments in the primary system due to the action of external virtual moment $X = 1$ in-lb/in. The moments are drawn on the compression side of the member. The functions indicated in the figure are defined as follows:

$$\overline{m}(y)_{k-1} = \overline{m}(y)_{k+1} = \frac{1b\ y}{2\ell}(L-y) \tag{25a}$$

and

$$\overline{m}(y)_k = \frac{1b\ y}{\ell}(L-y) \tag{25b}$$

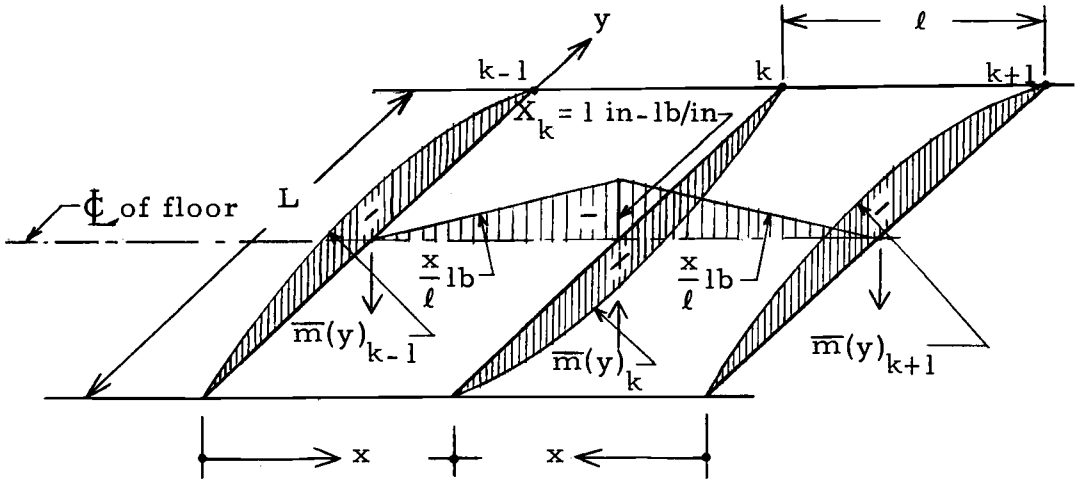

Figure 5. Internal moments due to virtual moment $X_k = 1$ in-lb/in.

Based on Equation 6 and Figure 5, $a_{k,k}$ is evaluated as follows:

$$a_{k,k} = \left[\int_x \overline{m}_f^2 \frac{dx}{EI_f}\right]_{\text{floor}} + \left[\int_y \overline{m}_k^2 \frac{dx}{EI_k}\right]_{\text{joists}}$$

$$= 2\int_{x=0}^{\ell} (L\ lb\ \frac{x}{\ell})^2 \frac{dx}{EI_f L} + \int_{y=0}^{L} \{[\overline{m}(y)_{k-1}]^2 \frac{1}{EI_{k-1}}$$

$$+ [\overline{m}(y)_k]^2 \frac{1}{EI_k} + [\overline{m}(y)_{k+1}]^2 \frac{1}{EI_{k+1}}\}dy \qquad (26)$$

Substituting Equations 25 into Equation 26 and integrating[2]:

$$a_{k,k} = \frac{2L\ell\ lb^2}{3EI_f} + \frac{lb^2\ L^5}{120\ell^2}\left(\frac{1}{EI_{k-1}} + \frac{4}{EI_k} + \frac{1}{EI_{k+1}}\right) \qquad (26a)$$

The following new terms are introduced:

$$A_f = \frac{L\ell\ lb^2}{6EI_f} \qquad (27a)$$

$$A_k = \frac{a}{EI_k} \qquad (27b)$$

$$A_{k+1} = \frac{a}{EI_{k+1}} \qquad (27c)$$

and

$$A_{k-1} = \frac{a}{EI_{k-1}} \qquad (27d)$$

[2]Refer to Appendix for development.

where

$$a = \frac{lb^2 L^5}{120\ell^2}$$

Substituting Equations 27 into Equation 26a:

$$a_{k,k} = 4(A_f + A_k) + A_{k-1} + A_{k+1} \tag{26b}$$

Coefficients $a_{k,k+1}$ are developed in the same manner as $a_{k,k}$ on the basis of internal virtual moments caused by external virtual unit moments applied at nodal locations k and $k+1$. They equal:

$$a_{k,k+1} = a_{k+1,k} = \left(\frac{L\ell\, lb^2}{6EI_f}\right) - \left(\frac{lb^2 L^5}{60\ell^2}\right)\left(\frac{1}{EI_k} + \frac{1}{EI_{k+1}}\right) \tag{28}$$

or

$$a_{k,k+1} = A_f - 2(A_k + A_{k+1}) \tag{28a}$$

Similarly:

$$a_{k,k+2} = a_{k+2,k} = \frac{lb^2 L^5}{120\ell^2 EI_{k+1}} = A_{k+1} \tag{29}$$

and

$$a_{k,j} = 0 \quad \text{if} \quad k + 3 \leq j \leq k - 3$$

The dimensions of the coefficient a are (in-lb).

NUMERICAL EXAMPLE

Floor Specifications

One of the test floor systems constructed in the Forest Research Laboratory, Oregon State University, was used to demonstrate the preceding developments on an actual structure.

Using the symbols defined in Figure 1, the system has the following specifications:

Geometry: $L = 184$ in, $\ell = 16$ in, $n = 17$

Joists: size, 2 x 10 inches; species, Western Hemlock; grade, utility

Floor: half-inch five-ply plywood sub-floor; species, Douglas fir; grade, C-D

Nailing of plywood to the joists: 8d common nails spaced 6 in along the plywood edges and 10 in at intermediate locations

Supports: unrestrained, simple.

To solve matrix Equation 15, the first and last joists in the system, denoted as numbers 0 and 18, are assumed to have infinite rigidity. The reasoning for such an assumption is as follows. If joist no. 0 were free to vibrate it would possess the value $\phi(y)_0$ (Figure 3), which would in turn generate the element β_{01}, which would

again increase the size of matrix $\underset{\sim}{\beta}$ by the order of one. The same consideration applies to joist no. 18. Therefore the size of matrices $\underset{\sim}{\beta}$, $\underset{\sim}{a}$, and $\underset{\sim}{\omega}_I$ would be 19 x 19. Since no elements of $\underset{\sim}{a}$ with either subscript equal to 0 or 18 can exist, all the elements of the first row and column, as well as the last row and column of matrix $\underset{\sim}{a}$ are equal to zero. Such a matrix is a singular one whose inverse cannot be determined, which would render matrix Equation 15 insoluble.

The error due to the above assumption is small and localized to the region at both ends of the floor.

Further Properties of Joists

Table 1 in Appendix II summarizes the following properties of joists:

Moment of Inertia

The moment of inertia of rectangular joists was determined by measuring the depth and breadth near the center point.

Modulus of Elasticity

The modulus of elasticity was established from bending tests of individual joists performed according to ASTM-Designation D 198-27 (1961), (1, p. 130-42).

Mass

The mass of each joist was obtained by weighing each individual unit before construction.

Further Properties of Plywood

Moment of Inertia

The plywood was placed so that the grain direction of the top, center, and lower laminations was at right angles to the length of the joists. In calculating the net moment of inertia (I_f), the two remaining intermediate plies were neglected, since their grain direction is perpendicular to the major bending stresses and hence they contribute little in the way of resistance (5, p. 11). Figure 6 shows a cross section of the plywood as used in the floor.

$$I_f = 0.00825 \text{ in}^4 \text{ per 1-in wide strip}$$

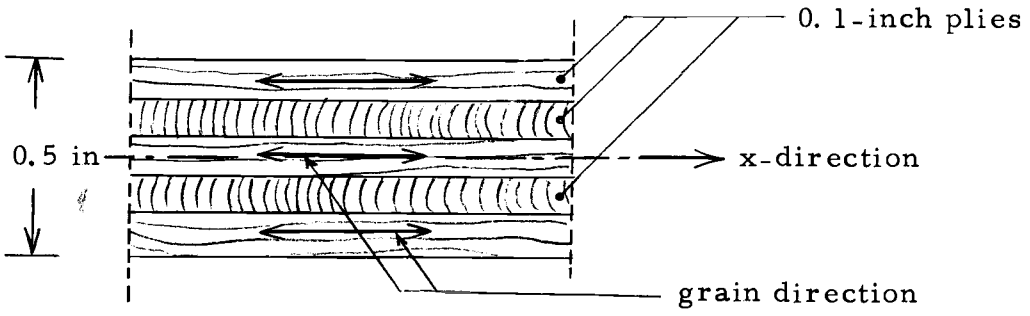

Figure 6. Cross-section of the plywood sheet.

Modulus of Elasticity

The major bending action in the plywood superstructure is about an axis parallel to the span of the joists. The plywood sheet acts as a slab on elastic supports, i. e., bending actions occur in two directions simultaneously, and hence double curvature will result. However, the curvature in the y-direction is prevented by the relatively rigid joists to which the sheet is nailed. Thus, the sheet deflects as a simple beam. The effective modulus of elasticity calculated from such deflection, hereinafter called the modulus of elasticity, is larger than the "pure" modulus in the same direction obtained on the basis of unrestrained deflection of the plywood sheet.

To determine the effective modulus of elasticity, five randomly selected plywood sheets were tested as shown in Figure 7. Five four-feet long dummy joists were nailed to the plywood in exactly the same way as for the floor system. A strip load of 1. 25 lb/in was applied along both four-feet edges. Deflection was measured at points 1, 2, and 3, from which the average deflection of each sheet Z_o was determined. The modulus of elasticity was calculated by the following formula:

$$E_f = \frac{wab^2c}{8I_f Z_o} \tag{30}$$

where all the symbols are apparent from Figure 7 or have already

been defined. Five test sheets generated a mean modulus of elasticity of

$$E_f = 1,908 \text{ ksi}$$

with a standard deviation of 37 ksi.

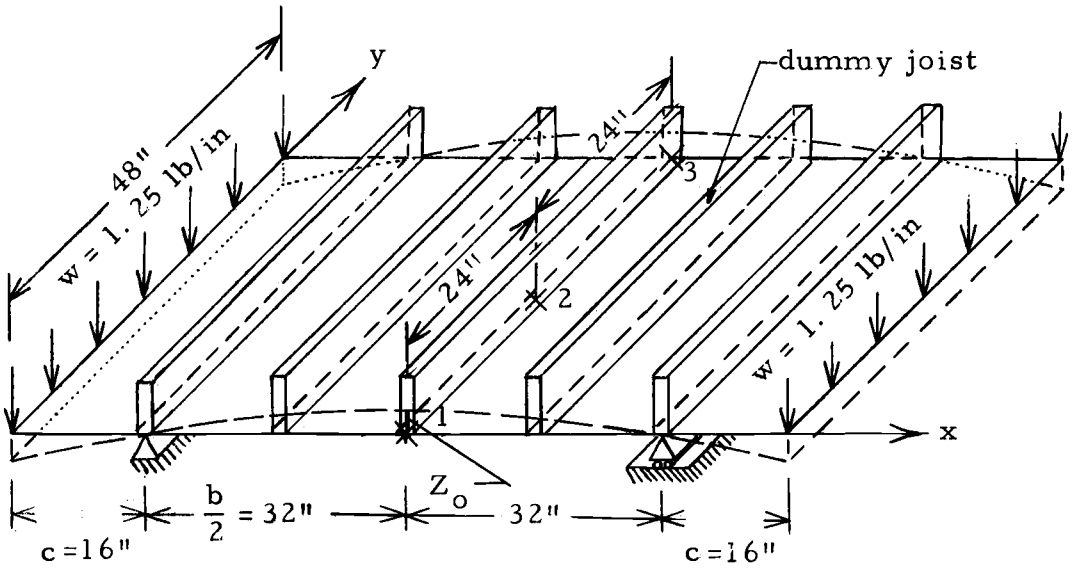

Figure 7. Test layout for modulus of elasticity of plywood sheet.

Mass

Ten randomly chosen plywood sheets were weighed, giving an average weight (W) of 44.1 lb per sheet. The mass per unit area was calculated as follows:

$$m_f = \frac{W}{Ag} = 0.2480 \times 10^{-4} \text{ lb sec}^2/\text{in}^3 \qquad (31)$$

where

$A = 32\ ft^2$ is area of plywood sheet

and $g = 32.16\ ft/sec^2$ is gravity acceleration.

Determination of Matrix $\underset{\sim}{\beta}$

Coefficients B were calculated by substituting numerical values of $L, \ell, E_f, I_f, m_f, EI_k, m_k$ and m_k' in Equations 19. The calculations were performed on the electronic Monro calculator, Epic 2000. This enabled the coefficients to be determined in one programmed operation. The values are given in Table 2 in Appendix II. These B values were substituted into Equations 18b, 20a, 21a, 22, and 23, which were evaluated on the aforementioned electronic calculator, so that all the non-zero elements of matrix $\underset{\sim}{\beta}$ were obtained. The elements of matrix $\underset{\sim}{\beta}$ are shown in Table 3 (Appendix II).

In calculating the elements of matrix $\underset{\sim}{\beta}$, the following aspect was taken into consideration. Since the alternate plywood sheets as shown in Figure 1 are butt-jointed at joists no. 3, 6, 9, 12 and 15, the virtual unit moment $X_k = 1$ in-lb/in applied at the above nodal locations acts only over half the span. Thus all the elements of columns 3, 6, 9, 12 and 15 in matrix $\underset{\sim}{\beta}$ are in reality one-half of those values obtained from Equations 18b, 20a, 21a, 22, and 23. Matrix $\underset{\sim}{\beta}$ written in a proper form would be obtained by substituting the appropriate values of Table 3 into Equation 7c.

Determination of Matrix $\underset{\sim}{a}$

The values of the coefficients of A were calculated by substituting numerical values for $L, \ell, E_f, I_f, E_k,$ and I_k into Equations 27. The resulting values were further substituted into Equations 26b, 28a, and 29, so that all the non-zero elements of matrix $\underset{\sim}{a}$ were obtained. As before, all the calculations were performed on the electronic calculator. The elements of matrix $\underset{\sim}{a}$ are shown in columns 2 to 6, Table 4 (Appendix II). The proper form of the matrix $\underset{\sim}{a}$ may be obtained by substituting the values of Table 4 into Equation 8b.

As in the calculation of matrix $\underset{\sim}{\beta}$, partial discontinuity at nodal locations 3, 6, 9, 12, and 15 has to be accounted for. Since both subscripts of the elements of $\underset{\sim}{a}$ denote the location of the action of external virtual unit moments, all the elements of both rows and columns 3, 6, 9, 12, and 15 equal one-half of those obtained by Equations 26b, 28a, and 29.

Determination of Matrix $\underset{\sim}{\omega}_I$

Considering the fundamental mode of joist k only, the square of Equation 2 becomes:

$$\omega^2_{k,k} = \frac{\pi^4}{L^2} \frac{EI_k}{m_k'} \qquad (32)$$

The elements of matrix $\underset{\sim}{\omega}_I$ shown in column 7, Table 4 are

obtained by substituting the values for $L, E_k, I_k,$ and m_k' into Equation 32. The proper form of matrix $\underset{\sim}{\omega}_I$ could be obtained by substituting the values of column 7, Table 4 into Equation 8a.

Solution of the Frequency Equation

Matrix Equation 15 was solved using the high speed digital computer. The computation and the programming were performed by the Computer Center, Oregon State University. Both the matrix operations and the solution for characteristic values were performed in only one operation. The program can be extended by adding to it a subprogram for determination of the matrices $\underset{\sim}{\alpha}$, $\underset{\sim}{\beta}$ and $\underset{\sim}{\omega}_I$.

The resulting frequencies of the floor system are shown in column 3 of Table 5, Appendix II. They are arranged in ascending order where individual rows represent the modal numbers.

Comparison of Calculated and Test Results

Since the analyzed floor system has the same specifications as the test one, the calculated frequencies are compared to those obtained from the tests.

Brief Description of the Testing Procedure

The floor system initially deflected by a 200 lb load applied at the floor center was allowed to vibrate freely when the load was

suddenly taken off the floor. Linear variable differential transformers, with movable cores attached to the bottom of each joist and coils fixed to the permanent base, were used as transducers. A signal was amplified and recorded in an oscillograph calibrated in such a way that time versus deflection traces were obtained.

Evaluation of Test Results

Most of the time-deflection plots obtained by testing are of a compound nature, with two or more modes combined into one complex trace, as may be seen in Figure 8. Since such a trace cannot be broken into simple modes by simple observation or reading, the following approximation is taken into consideration. Those regions on the trace which have a smooth shape similar to the sine curve, such as regions I and II in Figure 8, are selected. It is thought that either one mode only, or two or more modes with frequencies of similar magnitude act in these regions.

Some values determined as described above may be in error and some may not even appear isolated enough to be recognized. Those frequencies that could be obtained are shown in column 4 of Table 5. The mode of each frequency obtained from the test was determined by comparing it to the closest calculated frequency. Column 5, Table 5, lists the periods (T) in seconds per cycle determined directly from the test curves.

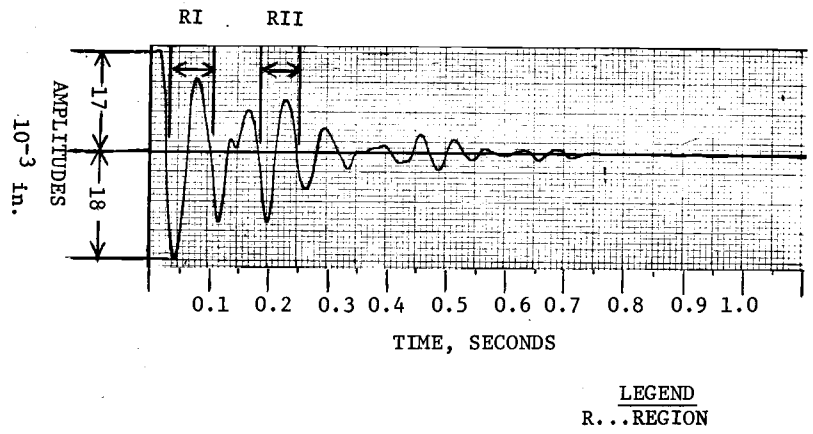

Figure 8. Example of time-deflection trace of freely vibrating floor system.

Comparison

Column 2 of Table 5 shows the frequencies of the primary system. The difference between the values in columns 2 and 3 is due to the action of redundant moments in the floor. There is a good correspondence between the calculated values and those obtained from the tests, as shown in columns 3 and 4 of Table 5. The largest discrepancy, which occurs at the first mode, is less than 2%.

CONCLUSIONS

The procedure applied and further developed in this work may be used to determine the natural frequencies of joist floors of any kind: timber, concrete, steel or composite types. Equation 15 applies to all of them, while the expressions for the elements of matrices $\underset{\sim}{\alpha}$ and $\underset{\sim}{\beta}$ may be used in all cases with insignificant bending action along the joists.

BIBLIOGRAPHY

1. American Society for Testing and Materials. 1967 book of ASTM standards. Part 16. Philadelphia, 1967. 896 p.

2. Biggs, John M. Introduction to structural dynamics. New York, McGraw-Hill, 1964. 341 p.

3. Bleich, Hans H. Frequency analysis of beam and girder floors. Transactions of the American Society of Civil Engineers 114: 1023-1063. 1949.

4. Bois, Petit G. Tables of indefinite integrals. New York, Dover, 1961. 150 p.

5. Douglas Fir Plywood Association. Douglas Fir Plywood (Pseudotsuga taxifolia) manufactured and graded under rules and supervision of Douglas Fir Plywood Association. Rev. ed. Tacoma, 1940. 12 p. (Technical Bulletin no. 6)

6. International Conference of Building Officials. Uniform building code. Pasadena, 1967. 595 p.

7. Isaacs, David V. The structural sufficiency of domestic buildings. 2d ed. Sydney, Australia, 1950. 50 p. (Australia. Commonwealth Experimental Building Station. Bulletin no. 1)

8. Jacobson, Lydik S and Robert S. Ayre. Engineering vibrations. New York, McGraw-Hill, 1958. 564 p.

9. Laursen Harold I. Matrix analysis of structures. New York, McGraw-Hill, 1966. 155 p.

10. Parcel, John I. and Robert B. B. Moorman. Analysis of statically indeterminate structures. New York, John Wiley, 1955. 571 p.

11. Pradko, F., Richard Lee and Victor Kaluza. Theory of human vibration response. New York, American Society of Mechanical Engineers, 1966. 12 p. (ASME publication no. 66-WA/BHF-15)

12. Reiher, H. and F. J. Meister. The sensitiveness of the human body to vibrations. Forschung auf dem Gebiete des Ingenieurwesens 2:381-386. 1931. (Translated in U. S. Air Materiel Command. Translation no. F-TS-616-RE. 1946. 15 p.)

13. Russel, William A. Deflection characteristics of residential wood-joist floor systems. Washington, D. C., U. S. Housing and House Finance Agency, 1954. 64 p. (Housing Research Paper no. 30)

14. Voltera, Enrico and E. C. Zachmanoglou. Dynamics of vibrations. Columbus, Charles E. Merril, 1965. 622 p.

APPENDICES

APPENDIX I

Sample Calculations

Development of Coefficients $\beta_{k,k}$

$$\beta_{k,k} = \int_{x=0}^{\ell}\int_{y=0}^{L}\left(\sqrt{\frac{2}{L}}\sin\frac{\pi y}{L}\right)\left[\frac{y\,1b}{\ell\,24}(L^3-2Ly^2+y^3)\right]\left(\sqrt{\frac{1}{m_k'}}\right)\frac{x}{\ell}\left\{\frac{1}{EI_{k-1}}\right.$$

$$\left.-\frac{1}{EI_{k-1}}+\frac{2}{EI_k}\right]\frac{x}{\ell}+\frac{1}{EI_{k+1}}-\left[\frac{1}{EI_{k+1}}+\frac{2}{EI_k}\right]\frac{x}{\ell}\Big\}m_f\,dx\,dy$$

$$+\int_{x=0}^{\ell}\int_{y=0}^{L}\left(\sqrt{\frac{2}{L}}\sin\frac{\pi y}{L}\right)\left(\sqrt{\frac{1}{m_k'}}\right)\frac{x}{\ell}\left[\frac{2\,1b}{6EI_f}(\ell x-\frac{x^3}{\ell})\right]m_f\,dx\,dy$$

$$+\int_{y=0}^{L}\left(\sqrt{\frac{2}{L}}\sin\frac{\pi y}{L}\right)\left(\sqrt{\frac{1}{m_k'}}\right)\left[\frac{y\,1b}{24\ell}(L^3-2Ly^2+y^3)\right]\left(\frac{-2}{L^5I_k}\right)m_k\,dy$$

$$=\sqrt{\frac{2}{m_k'L}}\left\{\int_{x=0}^{\ell}\left[\frac{x}{\ell}\left(\frac{1}{EI_{k-1}}+\frac{1}{EI_{k+1}}\right)-\frac{x^2}{\ell^2}\left(\frac{1}{EI_{k-1}}+\frac{4}{EI_k}+\frac{1}{EI_{k+1}}\right)m_f\,dx\right.\right.$$

$$\left.-\frac{2m_k}{EI_k}\right]\left(\frac{1b}{24\ell}\right)\int_{y=0}^{L}y(L^3-2Ly^2+y^3)\left(\sin\frac{\pi y}{L}\right)dy$$

$$\left.+\left(\frac{1b}{3EI_f}\right)m_f\int_{x=0}^{\ell}\left(x^2-\frac{x^4}{\ell^2}\right)dx\int_{y=0}^{L}\sin\frac{\pi y}{L}\,dy\right\} \qquad (A-1)$$

The following integral was evaluated from integral tables (4, p. 116):

$$\int_{y=0}^{L}y(L^3-2Ly^2+y^3)\left(\sin\frac{\pi y}{L}\right)dy = 0.156852L^5 \qquad (A-2)$$

and

$$\int_{y=0}^{L} (\sin \frac{\pi y}{L}) dy = \frac{2L}{\pi} \qquad (A-3)$$

Integrating expression A-1 between $x = 0$ and $x = \ell$ and substituting Equations A-2 and A-3 into Equation A-1 gives:

$$\beta_{k,k} = \sqrt{\frac{2}{m_k' L}} \left\{ [\frac{1}{2}(\frac{1}{EI_{k-1}} + \frac{1}{EI_{k+1}}) - \frac{1}{3}(\frac{1}{EI_{k-1}} + \frac{4}{EI_k} + \frac{1}{EI_{k+1}}) m_f \ell \right.$$

$$\left. - \frac{2m_k}{EI_k \ell}](0.156852 L^5) + (\frac{1b\, m_f}{3EI_f})(\frac{2\ell^3}{15})(\frac{2L}{\pi}) \right\}$$

$$= (9.245621)(10^{-3}) 1b \sqrt{\frac{L}{m_k'}} \left\{ L^4 [\frac{m_f}{6}(\frac{1}{EI_{k-1}} + \frac{1}{EI_{k+1}} - \frac{8}{EI_k}) - (\frac{2m_k}{\ell EI_k})] \right.$$

$$\left. + (4.329265) \frac{m_f \ell^3}{EI_f} \right\}$$

which is identical to Equation 18a.

Development of Coefficients $a_{k,k}$

Substituting Equation 25 into Equation 26 gives:

$$a_{k,k} = 2 \int_{x=0}^{\ell} L (1b \frac{x}{\ell})^2 \frac{dx}{EI_f} + \left\{ \int_{y=0}^{L} [\frac{1b\, y}{2\ell}](L-y)]^2 dy \right\} [\frac{1}{EI_{k-1}} + \frac{4}{EI_k} + \frac{1}{EI_{k+1}}]$$

$$= \frac{2L\ell\, 1b^2}{3EI_f} + \frac{1b^2 L^5}{120\ell^2} (\frac{1}{EI_{k-1}} + \frac{4}{EI_k} + \frac{1}{EI_{k+1}})$$

which is identical to Equation 26a.

APPENDIX II

Tables

Table 1. Properties of joists.

k	E ksi	I in^4	m x 10^{-4} lb sec in^{-2}	m' x 10^{-4} lb sec in^{-2}
0	1,650	108.667	6.2708	10.2361
1	1,736	112.550	6.1875	10.1528
2	1,944	106.773	6.2708	10.2361
3	1,608	108.871	5.8333	9.7986
4	1,227	104.400	5.3958	9.3611
5	1,693	107.663	6.8889	10.8542
6	1,616	103.782	5.7917	9.7570
7	1,355	105.918	5.7431	9.7084
8	1,274	107.735	6.0556	10.0209
9	1,719	112.103	6.6250	10.5903
10	2,062	104.907	6.6667	10.6320
11	1,078	113.120	7.0208	10.9861
12	1,758	101.397	7.4097	11.3750
13	1,761	109.082	5.4792	9.4445
14	1,462	110.922	7.1042	11.0695
15	1,497	105.710	6.6667	10.6320
16	1,541	105.681	6.0972	10.0625
17	1,976	108.304	7.1458	11.1111
18	1,731	116.762	7.3681	11.3334

Table 2. Coefficients B.

k	b	$(B_{k,k})10^{-4}$	$(B_{k,k+1})10^{-4}$	$(B_{k,k-1})10^{-4}$	$(B_{k,f})10^{-4}$
1	1.8641	25.4853	0.8981	1.0396	1.0994
2	1.8565	24.1174	1.0604	0.9501	1.0949
3	1.8975	27.7923	1.4812	0.9141	1.1191
4	1.9413	36.8542	1.0650	1.1089	1.1449
5	1.8028	28.5196	1.0750	1.4074	1.0633
6	1.9015	28.9298	1.3249	1.0432	1.1215
7	1.9063	28.8350	1.3889	1.1366	1.4243
8	1.8698	35.8480	0.9703	1.3028	1.1028
9	1.8252	26.5539	0.8437	1.3298	1.0764
10	1.8216	23.7150	1.4938	0.9453	1.0743
11	1.7920	42.9590	1.0053	0.8284	1.0569
12	1.7611	30.0430	0.9168	1.4442	1.0386
13	1.9327	24.7215	1.1918	1.0842	1.1399
14	1.7852	32.4589	1.1281	0.9293	1.0529
15	1.8216	32.4173	1.1185	1.1233	1.0743
16	1.8724	30.3994	0.8749	1.1832	1.1043
17	1.7819	24.6549	0.8816	1.0941	1.0509

Table 3. Elements of matrix β_{ik}

k	Dimensions: $(10^{-3})(in^{1/2}lb^{1/2}sec)$				
	$\beta_{k,k}$	$\beta_{k,k+1}$	$\beta_{k,k-1}$	$\beta_{k,k+2}$	$\beta_{k,k-2}$
1	-2.2448	1.1496	0	0.0449	------
2	-2.1012	0.5243	1.0706	0.1060	0
3	-1.2139	1.1493	1.2627	0.1481	0.0914
4	-3.3535	1.6870	0.8391	0.0533	0.1109
5	-2.4974	0.6321	1.1977	0.1075	0.0704
6	-1.2720	1.2376	1.2939	0.1325	0.1043
7	-2.5185	1.2202	0.6353	0.0694	0.1137
8	-3.2472	0.8267	1.5870	0.0970	0.0651
9	-1.1652	1.2128	1.1156	0.0844	0.1330
10	-2.0202	0.9407	0.5252	0.0747	0.0945
11	-4.0069	0.9999	2.0351	0.1005	0.0414
12	-1.3322	1.3707	1.2653	0.0917	0.1444
13	-2.1306	1.0547	0.5381	0.0596	0.1084
14	-2.9349	0.7250	1.4897	0.1128	0.0465
15	-1.4551	1.4509	1.4499	0.1119	0.1123
16	-2.7237	1.4002	0.6693	0	0.1183
17	-2.1628	0	1.0665	------	0.0547

Table 4. Elements of matrices $\underset{\sim}{a}$ and $\underset{\sim}{\omega}_I$.

k	Dimensions: 10^{-2} in-lb					
	$a_{k,k}$	$a_{k,k+1}$	$a_{k,k-1}$	$a_{k,k+2}$	$a_{k,k-2}$	$\omega^2_{k,k}$
1	2	3	4	5	6	7
1	33.6622	-10.5250	--------	1.6538	------	16,355
2	33.1362	- 5.6704	-10.5250	3.9217	------	17,233
3	18.4121	- 7.7223	- 5.6704	2.6797	1.6538	15,183
4	41.5966	-15.1345	- 7.7223	1.8833	3.9217	11,629
5	36.9898	- 6.3013	-15.1345	4.0936	2.6797	14,271
6	18.6975	- 7.3184	- 6.3013	2.3918	1.8833	14,608
7	40.7006	-16.4536	- 7.3184	2.5010	4.0936	12,563
8	40.8248	- 7.0058	-16.4536	3.5627	2.3918	11,560
9	17.4485	- 5.1776	- 7.0058	1.5869	2.5010	15,464
10	34.3582	-14.4900	- 5.1776	2.8150	3.5627	17,290
11	42.0159	- 7.9227	-14.4900	3.8515	1.5869	9,433
12	18.5402	- 5.8667	- 7.9227	1.7870	2.8150	13,317
13	34.8515	-12.4975	- 5.8667	2.1168	3.8515	17,285
14	37.3171	- 7.0131	-12.4975	4.3384	1.7870	12,450
15	19.1367	- 6.9953	- 7.0131	2.1079	2.1168	12,497
16	36.8797	-11.7298	- 6.9953	------	4.3384	13,754
17	32.9151	--------	-11.7298	------	2.1079	16,368

Table 5. Natural frequencies.

Modes	Frequencies, cps			Period test values sec/cycle
	Primary system	Floor system		
		Calculated values	Test values	
1	2	3	4	5
1	15.439	12.947	13.2	0.076
2	17.111	14.449	14.3	0.070
3	17.162	14.519		
4	17.761	14.887	14.9	0.067
5	17.793	15.476	15.6	0.064
6	17.839	16.119	16.1	0.062
7	18.368	16.387	16.4	0.061
8	18.665	16.641	16.7	0.060
9	19.013	17.071	17.0	0.059
10	19.236	17.161	17.2	0.058
11	19.612	17.937	17.9	0.056
12	19.793	18.247	18.2	0.055
13	20.256	18.711		
14	20.263	19.062	18.9	0.053
15	20.892	19.638	19.6	0.051
16	20.925	19.942		
17	20.929	20.182		